RANS COMPUTATIONS OF FLOW AROUND A BULK CARRIER WITH ENERGY SAVING DEVICE

Charles E. Badoe , Arun P. Lakshmynarayanana, Artur K. Lidtke, Josef Camilleri, Alexander B. Phillips, Joseph Banks, Stephen R. Turnock

Fluid Structure Interactions Research Group, Faculty of Engineering and the Environment, University of Southampton, UK

SUBMISSION EXPLANATION

Test cases: Case 1.3, 1.4 and 1.7

Name of Code: OpenFOAM and Star-CCM+

Institution::University of Southampton, UK

MODELING

Governing Equations: Single-phase Steady Reynolds Averaged Navier-Stokes (RANS)equations

Turbulence Modeling: Shear Stress Transport (Isotropic two equation blended $k\omega/k\varepsilon$ model (Menter 1994))

Propeller Models: Prescribed body force approach (Badoe *et al.*, 2012).

NUMERICAL METHOD

Discretization: RANS equations were solved with both codes on a body-fitted multi block structured grid by means of cell centered finite volume method (FVM). Discretisation of the convection terms were achieved using Gauss linear second order upwind and the diffusion terms were treated using the central difference scheme. First-order schemes were applied to the turbulent quantities.

Velocity-Pressure Coupling: Semi Implicit Method for Pressure Linked Equations(SIMPLE) algorithm.

HIGH PERFORMANCE COMPUTING

Iridis 4 Linux Cluster (University of Southampton)

64 Partitions run on 4, 16 processor nodes (OpenFOAM)

64 Partitions run on 4, 16 processor nodes (Star-CCM+)

Simulation time: Approximately 12 wall clock hours for OpenFOAM self propulsion computations and xxxxxxx for Star-CCM+ self-propelled computations.

Grids, Domain, Boundary and Flow Conditions

Grids: Structured, hexahedral meshes created using pointwise were used for both Star-CCM+ and OpenFOAM. All grids were designed with y+<1 over the entire surface of the ship. Particular challenge in the mesh design was to accommodate the energy saving device without causing strong non-orthogonality of the cells whilst meeting the wall-normal cell size requirements. An outline of the final configuration, showing the definition of individual mesh blocks is shown in Fig. 1. Resolving the vortical structures onset to the propeller plane also required sufficient mesh density in the outer boundary layer regions near the stern, as shown in Fig. 2 for measurement station 4 with (left) and without (right) the ESD, respectively. Total cell counts used in the considered grids is shown in Table 1.

Fig.1: Structure of the final mesh around the JBC hull with duct, showing local refinement regions near hull, near duct and in the wake regions.

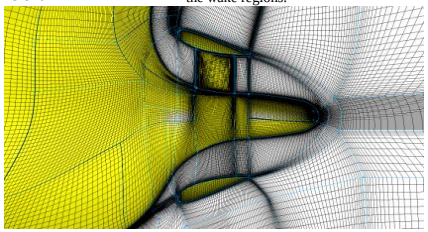

Domain: Size matches the NMRI towing tank dimensions in [Y, Z] and extend 1.5Lpp upstream and 3.5Lpp downstream of the hull.

Boundary Conditions: No-slip walls on all geometries, sides and bottom of domain treated with slip condition and symmetry plane ensured on atmospheric boundaries.

Grid	Size
Coarse without ESD	4.03M
Fine without ESD	9.72M
Fine with ESD	10.63M

Table 1: Grids used for computations(cell counts quoted for half body)

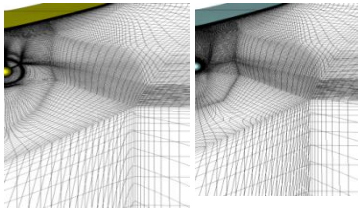

Fig. 2: Structure of the final mesh around the propeller plane and wake region with (left) and without (right) the ESD.

Results

Resistance: Table 2 compares the total towed resistance with and without ESD between Star-CCM+ and OpenFOAM. Due to the low operating Froude number of the JBC (Fn= 0.142), wave resistance was neglected in all computations.

Flow pattern: Limiting streamlines on the hull surface are shown in Fig. 3 for the OpenFOAM simulations. Without the duct present the flow coming from underneath the ship may be seen to separate around the area of high curvature (shown as area B). Higher above the keel the flow may be seen to approach the separation zone from the top. A secondary separation zone may be seen between points A and C and further downstream along the shaft line and the hub. This is most likely associated with the flow from the upper parts of the hull encountering high curvature. Flow divergence can also be seen at the saddle point (marked as D). Addition of the duct may be seen to significantly reduce the size of the separation zone associated with separation from the bilge by virtue of inducing a more favourable pressure gradient. Vortical structures for the case without duct in Fig 4 show a strong vortex at the propeller plane due to separation from the bilge downstream of the aft shoulder, confirming the observations drawn from analysing the limiting streamlines.

Axial velocity plots: Towed condition with duct using the both codes is shown in Fig. 5. In general, there was very little difference between the flow field generated by both codes. A less intense bilge vortex is predicted using the SST k-ω model compared with the experiments. Star-CCM+ (Fig 9) showed much improved wake behind the duct.

Parameter	EFD	OpenFOAM	StarCCM+
Without ESD			
$C_T \times 10^3$	4.289	4.318	4.196
$C_F \times 10^3$		3.328	3.244
$C_P \times 10^3$		0.990	0.952
With ESD			
$C_T \times 10^3$	4.263	4.259	4.246
$C_F \times 10^3$		3.314	3.273
$C_P \times 10^3$		0.946	0.970

Table 2: Summary of ship resistance prediction with and without ESD (final grid)

Fig 3: Limiting streamlines without/with ESD using OpenFOAM

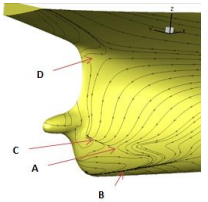

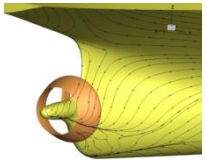

Fig 4: Vortical structures without/with ESD using OpenFOAM

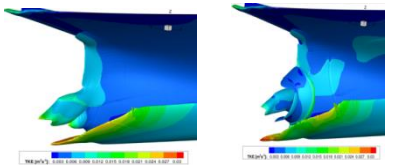

Self-propulsion: Results are presented in Fig. 6. An important observation was the effect of the ESD boundary layer on the predicted and measured axial velocity contours. This is not visible in the OpenFOAM case, however. The reason is that the Star-CCM+ simulation used an all y+ boundary layer model, whereas the open-source counterpart fully resolved the boundary layer. Due to a very low Reynolds number of the duct (25000 based on chord and free-stream velocity) the more explicit approach does not yield satisfactory results. On the other hand, the wall-function approach leads to duct wake being seen around top-dead centre, which is not seen in the experiment.

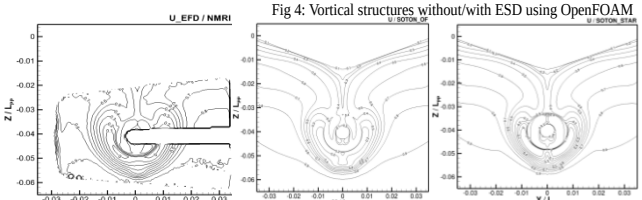

Fig 5: Results of mean axial velocity at x/Lpp = 0.9843with ESD in the towed condition. Experiment (left), OpenFOAM (middle), StarCCM+ (right).

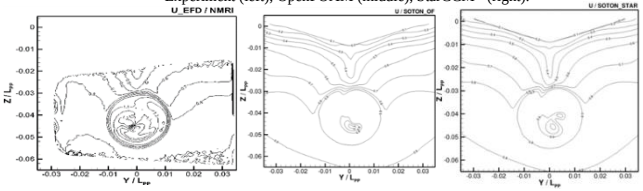

Fig 6: Mean axial velocity at x/Lpp = 0.9843 without ESD in the self-propelled condition. Experiment (left), OpenFOAM (middle), StarCCM+ (right).

REFERENCES

Badoe, C., Phillips, A.B. and Turnock, S.R., (2012), Initial numerical propeller rudder interaction studies to assist fuel efficient shipping, in 'Proceedings of the 15th Numerical Towing Tank Symposium, 7-9 October, Cortona Italy' 36(15-16), pp.1217-1225.

Menter, F.R., 1994. Two-equation eddy viscosity turbulence models for engineering applications. AIAA journal, 32(8), pp.1598–605.